



# Organic aerosol sources in the Milan metropolitan area – Receptor modelling based on field observations and air quality modelling

K.R. Daellenbach<sup>a,\*</sup>, M. Manousakas<sup>a</sup>, J. Jiang<sup>a,b</sup>, T. Cui<sup>a</sup>, Y. Chen<sup>a</sup>, I. El Haddad<sup>a</sup>, P. Fermo<sup>c</sup>, C. Colombi<sup>d</sup>, A.S.H. Prévôt<sup>a</sup>

<sup>a</sup> Laboratory of Atmospheric Chemistry, Paul Scherrer Institute (PSI), 5232, Villigen-PSI, Switzerland

<sup>b</sup> Shanghai Key Lab for Urban Ecological Processes and Eco-Restoration, School of Ecological and Environmental Sciences, East China Normal University, 200241, Shanghai, China

<sup>c</sup> Dipartimento di Chimica, Università degli Studi di Milano, 20133, Milan, Italy

<sup>d</sup> Regional Agency for Environmental Protection of Lombardy (ARPA Lombardia), Air Quality Department, 20124, Milan, Italy

## HIGHLIGHTS

- We identify the organic aerosol sources in Milan, a pollution hotspot in Europe.
- Residential heating (wood) governed wintertime OA throughout the last decade.
- In winter, secondary OA is mainly produced by residential wood burning emissions.
- In summer, secondary OA is formed both from biogenic and anthropogenic emissions.

## ABSTRACT

The Milan metropolitan area in Northern Italy experiences historically severe particulate matter pollution episodes characterized by high organic aerosol (OA) concentrations. However, the main sources of OA, especially atmospherically formed secondary OA (SOA) are not well understood. Here, we investigated the emission sources contributing to the directly emitted OA (Primary – POA) and to the SOA in urban Milan, where such information is particularly lacking. We used advanced mass spectrometric analytical techniques for the characterization of archive samples, as well as statistical receptor modeling (positive matrix factorization, PMF) and air quality modeling, to establish a base case for investigating the time evolution of source contributions. We found that residential heating biomass burning POA (BBOA) were a major detrimental factor for air quality during the winter (37% of OA, under polluted conditions up to 56% of OA). Inefficient combustion conditions identified by high BBOA/K<sup>+</sup> ratios contributed to the high relative contribution of BBOA to OA. Long-term tracer analyses suggest that BBOA concentrations remained approximately constant over the last decade (2012–2022), supporting the conclusion that emissions from biomass burning remained a major driver of winter-time OA pollution. Yet assessing changes in the contribution of other OA sources require future research. While POA emissions were the most important contributor to OA during winter (62% of OA), SOA dominated OA during summer (62% of OA). Our combined advanced mass spectral source apportionment and air quality modelling analyses indicated that winter-time SOA were mostly affected by biomass burning related precursor emissions, while summer-time SOA were linked to both the remaining anthropogenic emissions (industry, energy production, shipping, and traffic) and to biogenic emissions. Altogether, this study quantified the major emission sources of OA and thus provides crucial information about OA sources and a baseline for comparison to the present situation which is needed for tackling OA pollution in one of the major pollution hotspots in Europe. Overall, this study presents a transferable framework combining chemical source apportionment with bottom-up air quality OA source analyses in order to better understand the formation of SOA.

## 1. Introduction

While air quality in Europe has improved during the last decades, certain regions are still highly polluted (EEA, 2016; Chen et al., 2022; Daellenbach et al., 2020). One of these European air pollution hotspot regions is the Po basin, especially, the Milan metropolitan area (Jiang et al., 2019; Daellenbach et al., 2020). This region in Northern Italy

experiences historically - mostly in winter - severe particulate matter pollution episodes. A large mass fraction of PM<sub>10</sub> (particles with aerodynamic diameter <10 µm) is organic – termed organic aerosol (OA) (Jimenez et al., 2009; Putaud et al., 2010; Bressi et al., 2021; Chen et al., 2022). In part, OA is directly emitted as particles –primary OA (POA) - and in part formed via atmospheric chemical processing of volatile organic compounds (VOCs) –secondary OA (SOA) (Hallquist et al.,

\* Corresponding author.

E-mail address: [kaspar.daellenbach@psi.ch](mailto:kaspar.daellenbach@psi.ch) (K.R. Daellenbach).

<https://doi.org/10.1016/j.atmosenv.2023.119799>

Received 11 January 2023; Received in revised form 11 April 2023; Accepted 18 April 2023

Available online 14 May 2023

1352-2310/© 2023 The Authors. Published by Elsevier Ltd. This is an open access article under the CC BY license (<http://creativecommons.org/licenses/by/4.0/>).

2009). OA is the least well understood of the main PM constituents (e.g. Amato et al. (2016)), because the complex chemical composition of OA hinders reaching the same level of understanding as for the other constituents without using advanced chemical characterizations. Major progress over the last two decades has improved the knowledge of the sources of POA substantially, yet the sources and formation pathways of SOA are to the largest extent still unknown on a global scale. Particularly, in polluted urban areas, the presence of a multitude of emission sources create extremely complex SOA mixtures (Sun et al., 2018; Bhandari et al., 2022; Huang et al., 2014; Chen et al., 2020; Ma et al., 2022; Wang et al., 2017; Mehra et al., 2021; Qi et al., 2019; Kumar et al., 2022; Tong et al., 2021). This is of particular relevance because SOA is the main contributor to OA and PM in most regions (Jimenez et al., 2009; Chen et al., 2022). Knowledge of the main emission sources driving PM levels is essential for stakeholders, both to define appropriate pollution reduction strategies and to evaluate their effectiveness. The assessment of the mitigation policies is possible only by investigating the evolution of the emissions over a considerable period of time.

In addition, the chemical composition of PM is thought to determine its adverse health effects (Bates et al., 2019; Gao et al., 2020; Valavanidis et al., 2008; Ostro et al., 2011). Therefore, a detailed understanding of the emission sources of PM, which are strongly affecting the chemical composition of the particles, is essential for mitigating health effects. Field observations of the chemical composition of OA – in line with air quality modelling – suggest that residential heating biomass burning emissions were and still are an important contributor to OA in the Po basin in addition to road traffic POA (Gilardoni et al., 2016; Paglione et al., 2014, 2020; Bressi et al., 2016; Pietrogrande et al., 2014a, 2014b; Jiang et al., 2019; Amato et al., 2016). Beyond the impact of biomass burning emissions on SOA formation during the cold season, the impact of other anthropogenic but also natural emission sources is, to the largest degree, unknown, especially during the rest of the year. This is even further pronounced for the Milan metropolitan area – the population center of the region – for which studies on the sources of OA overall are lacking, both present and past. Here, we characterize for the first time the sources of POA and SOA at an urban background location in Milan in the entire year 2013 via detailed filter-based aerosol mass spectrometry and air quality modeling for assessing seasonal variations in POA and SOA sources. This study is important not only because the POA and SOA sources are investigated in Milan, but it also provides a baseline for comparison to the present situation, which is necessary for implementing and assessing mitigation policies. A novel approach of combining the source apportionment results to modelling results was used to gain, for the first time in the region, insight into the precursor emissions that affect the formation of SOA during each season. This study is a unique combination of a highly advanced and rare analytical approach, an advanced source apportionment analysis and a novel use of air quality modelling results combined with source apportionment results.

## 2. Materials and methods

### 2.1. Study area and aerosol sampling

The urban background air quality monitoring station Milano-Pascal is one of the Italian Supersites (D. Lgs. 155/2010, Italian transposition of 2008/50/CE) and part of the Lombardia Air Quality Network of ARPA (Agenzia Regionale per la Protezione dell'Ambiente). The station is located inside a playground about 130 m from a road in the University area called “Città Studi” (45°28'44" N, 9°14'07" E) in Eastern Milan. At Milano-Pascal, long-term gaseous and particulate air quality observations have been running for years. The observations include meteorological information (relative humidity, temperature, precipitation, wind speed, and direction), gaseous pollutants (SO<sub>2</sub> via UV fluorescence, NO<sub>x</sub> via chemiluminescence, O<sub>3</sub> via UV photometry, NH<sub>3</sub> via chemiluminescence), PM<sub>10</sub> and PM<sub>2.5</sub> mass concentration (beta analyzers).

PM<sub>10</sub> was collected for standard chemical analysis by means of Low Volume Samplers on 47 mm diameter Teflon and Quartz filters from 2012 onward (US-EPA reference method samplers TECORA, 24 h collection from midnight to midnight). In addition, PM<sub>10</sub> was collected for offline aerosol mass spectrometry (AMS) analyses in 2013 by means of a High Volume Sampler on 14.7 cm diameter PallFlex QAT-UP quartz filters (Sequential High-Volume Sampler Digital DH80, 24 h collection from midnight to midnight). After collection, the filters were wrapped in aluminum foil and stored at –20 °C. Field blanks were collected following the same approach and used to correct the chemical analyses. The samples were protected against light and temperature between the sampling and the analysis, in conformity with EN15549 (European Committee for Standardization (CEN), 2008).

### 2.2. Chemical analysis of particulate matter

The chemical composition of the water-soluble organic aerosol in PM<sub>10</sub> was analysed using the offline AMS approach (Daellenbach et al., 2016; Mihara and Mochida, 2011) using HiVol Quartz fiber filter samples collected for 24-h on every 4th day (when available) during the entire year 2013. The analytical approach is analogous to Daellenbach et al. (2017). PM collected on the Quartz-fiber filters were extracted in water (milliQ, 18.2 MΩ cm, total organic carbon TOC <5 ppb, 25 °C), and the nebulized extracts were analysed as dried particles using a High-Resolution Aerosol Mass Spectrometer (HR-AMS, Aerodyne Research, Inc.) (Canagaratna et al., 2007). The resulting chemical fingerprints of WSOA were quantified by combining water-soluble carbon (WSOC) concentrations from a total organic carbon analyzer (catalytic oxidation and non-dispersive infrared detection of CO<sub>2</sub>) and the organic matter – to – organic carbon ratio (OM:OC) from the HR-AMS. These WSOA chemical fingerprints were used to quantify the sources of WSOA via source apportionment analysis and after further corrections accounting for the water-solubility of the identified sources, even OA sources (see below) (Daellenbach et al., 2016; Daellenbach et al., 2017; Canonaco et al., 2021; Vlachou et al., 2018; Casotto et al., 2022a; Casotto et al., 2022b; Bozzetti et al., 2016; Bozzetti et al., 2017a; Bozzetti et al., 2017b; Moschos et al., 2022; Huang et al., 2014).

Further, organic and elemental carbon (OC, EC) were determined by a thermo-optical transmission thermo-optical reflectance method with a Sunset OC/EC analyzer (Birch and Cary, 1996), following the NIOSH-like thermal-optical transmission protocol. Water-soluble ions (K<sup>+</sup>, Na<sup>+</sup>, Mg<sup>2+</sup>, Ca<sup>2+</sup>, NH<sub>4</sub><sup>+</sup>, SO<sub>4</sub><sup>2-</sup>, NO<sub>3</sub><sup>-</sup>, Cl<sup>-</sup>, Br<sup>-</sup>) were analysed using ion chromatography (Jaffrezo et al., 1998). Anhydrosugars (arabitol, mannitol, levoglucosan, mannosan, galactosan, and glucose) analysis was performed by a high-performance anion exchange chromatography (HPAEC) with pulsed amperometric detection (PAD) using ion chromatography (Metrohm 881) following Vicente et al. (2015). Polyaromatic hydrocarbons PAHs (B(a)P, B(a)A, B(b)F, B(j)F, B(k)F, I(1,2,3, c,d)P, dB(a,h)A) were quantified by gas chromatography with mass spectrometry detector (GC-MS, method ISO12884/2000, according to 2008/50/EC and 2004/107/CE) on selected filter samples covering the entire year 2013. The concentrations of trace elements (Al, Si, S, Cl, K, Ca, Ti, V, Cr, Mn, Fe, Ni, Cu, Zn, Br, Rb, Pb, Sr, Sn, Sb, Ba) were determined using a Panalytical Epsilon5 Energy Dispersive X-Ray Fluorescence (ED-XRF) system applied to Teflon PM<sub>10</sub> filters (Giannoni et al., 2015). The instrument uses a polarized X-ray beam that allows for a significant reduction of spectral background. The system was calibrated with a set of Micromatter standards and tested with NIST 2782.

### 2.3. Source apportionment

The use of receptor models in source apportionment studies of atmospheric particulate matter is common. These methods enable a quantitative assessment contributions of primary and secondary sources to PM and its constituents. The receptor models estimate the impact of various sources at a specific location based on environmental data

(concentration and chemical composition of PM). A mass balance equation (Hopke, 2003) can be used for a dataset of PM chemical speciation:

$$X_{ij} = \sum_{k=1}^N G_{ik} F_{kj} + e_{ij} \quad (1)$$

Where  $X_{ij}$  represents the concentration of the  $i^{\text{th}}$  sample in the  $j^{\text{th}}$  species,  $F_{kj}$  represents the mass fraction of the  $j^{\text{th}}$  species emitted from the  $k^{\text{th}}$  source, and  $G_{ik}$  represents the concentration of the  $k^{\text{th}}$  source in the  $i^{\text{th}}$  sample. If  $F_{kj}$  are known for all sources, the Chemical Mass Balance (CMB) model (Watson, 1984) can be used; however, this model requires experimental profiles for all major sources. When both  $F_{kj}$  and  $G_{ik}$  are unknown, equations are solved using factor analysis techniques such as Principal Components Analysis (PCA) (Thurston and Spengler, 1985; Henry and Hidy, 1979) and Positive Matrix Factorization (PMF) (Paatero and Tapper, 1994) (Equation (1)).

Here, the chemical OA fingerprints from the offline AMS approach are analysed with the multivariate receptor model positive matrix factorization as implemented in the Multilinear Engine 2 (ME-2) controlled by the Source Finder (SoFi) interface (Paatero, 1999; Canonaco et al., 2013, 2021). To investigate the repeatability of AMS measurements on PMF outputs, each filter sample was represented by 11 WSOA mass spectral repetitions on average. A corresponding preceding measured blank from nebulized ultrapure water was subtracted from each mass spectrum. The method used is described in detail by (Daellenbach et al., 2017). ME-2 allows the use of a priori information on the chemical composition of sources by using anchor profiles in F and allowing only a certain relative deviation from the anchor (termed a-value approach) (Canonaco et al., 2013). We used a priori information on the composition of hydrocarbon-like OA related to POA from liquid fossil fuel combustion (HOA, primarily traffic exhaust) and cooking POA (COA) in this study, based on profiles from (Crippa et al., 2013). Ions found in our dataset but not in the reference profiles for HOA and COA were deduced from published unit mass resolution (UMR) profiles (Ng et al., 2011 and Crippa et al., 2013c). This was accomplished by comparing the fraction of signal at a specific  $m/z$  in the UMR reference spectrum ( $f_{\text{UMR},m/z}$ ) to the fraction of signal of all ions at this  $m/z$  in the HR reference spectrum ( $f_{\text{HR},m/z}$ ). For such missing ions, the difference  $f_{\text{UMR},m/z} - f_{\text{HR},m/z}$  was used as an entry with an a-value of unity. In a preliminary analysis, we resolved six sources contributing to WSOA. In addition to the constrained HOA and COA, biomass burning POA (BBOA), sulfur-containing POA (SCOA), and oxygenated OAs (OOAs representing SOA) with seasonal separation has been identified using six factors. With more than six factors, OOA was further split into profiles that could not be environmentally explained. Therefore, we opted for using a six factor solution (validation of the number of factors in Figures SI 1-3). Further, an a-value sensitivity analyses was performed (independently varying the tolerated relative deviation from the constrained anchor profile for HOA and COA 0–100%, 500 seeds).

In order to quantify the sources of OA, we determined for each WSOA source a recovery ( $R_k$ , the WSOC-to-OC ratio) which largely reflects its water-solubility. To that purpose, we assumed that the sum of all WSOC sources ( $\text{WSOC}_k$ ) corrected with their recovery ( $R_k$ ) should be equal to the measured OC concentrations ( $\text{OC}_{\text{meas}}$ ):

$$\text{OC}_{\text{meas}} = \sum_k \frac{\text{WSOC}_k}{R_k} \quad (2)$$

We solved equation (2) as a multilinear regression to reconstruct an independent OC concentration time series from a Sunset OC/EC analyzer data. While  $R_{\text{BBOC}}$ ,  $R_{\text{LO-OOC}}$ ,  $R_{\text{MO-OOC}}$ , and  $R_{\text{SCOC}}$  were unknown and determined via equation (2), for  $R_{\text{HOC}}$  and  $R_{\text{COC}}$  a priori information from Daellenbach et al. (2016) were used. Since WSOC concentrations were not available for all days/filters, the factor time series were corrected from WSOC to OA sources ( $\text{OA}_k$ ) using the approach described in Daellenbach et al. (2017):

$$\text{OA}_k = \frac{\frac{\text{WSOC}_k}{R_k}}{\sum_k \frac{\text{WSOC}_k}{R_k}} * \text{OC} * (\text{OM} : \text{OC})_k \quad (3)$$

PMF solutions and  $R_k$  combinations were only accepted if the OA factors fulfilled criteria regarding their factor profiles and factor time series (HOA and COA a-value range of the retained solutions is presented in Figure SI 4). HOA and COA were required to have a low relative contribution of the fragment ions  $\text{CO}_2^+$  (OOA marker) and  $\text{C}_2\text{H}_4\text{O}_2^+$  (BBOA marker) expressed as fragment ion concentration per WSOA concentration of the respective source, i.e. as a mass fraction ( $f(\text{CO}_2^+) < 0.4$ ,  $f(\text{HOA}(\text{C}_2\text{H}_4\text{O}_2^+)) < 0.004$ ,  $f(\text{COA}(\text{C}_2\text{H}_4\text{O}_2^+)) < 0.01$ ) (Daellenbach et al., 2017). In addition, solutions were only accepted if HOA correlated with  $\text{NO}_2$  ( $p < 0.05$ ), HOA correlated better with  $\text{NO}_2$  than COA ( $p < 0.05$ ), and BBOA correlated with levoglucosan ( $p < 0.05$ ). Henceforth, we report the median solution of all retained solutions ( $R_k$  distributions in Figure SI 5, OC reconstruction in Figure SI 6, uncertainty of concentration time series in Figure SI 7).

#### 2.4. Air quality modelling

The Comprehensive Air quality Model with Extensions (CAMx) version 6.5 (Ramboll, 2018) was used to simulate the components of particulate matter from different sources in the Milan metropolitan area. CAMx is a state-of-the-science chemical transport model over spatial scales ranging from neighborhoods to continents. The spatial resolution in this study is  $0.125^\circ \times 0.25^\circ$ , with 14 vertical layers ranging from ~20 to 7000 m above sea level. A modified volatility basis set (VBS) scheme (Jiang et al., 2019, 2021) was adopted to simulate the organic aerosols from different sources, while the partitioning of inorganic aerosols was modeled by the ISORROPIA thermodynamic model (Nenes et al., 1998). The emission inputs were obtained from the high-resolution European emission inventory CAMS-REG-v4 (Copernicus Atmosphere Monitoring Service-Regional inventory-version 4) at  $0.1^\circ$  resolution, developed by TNO (Netherlands Organization for Applied Scientific) (Kuenen et al., 2022). Details about other parameterizations and model inputs can be found in the literature (Jiang et al., 2019, 2021).

The model performance of CAMx on predicting air quality in Europe was validated in detail in previous studies (Jiang et al., 2019; Daellenbach et al., 2020), by comparing with the measurements of the major air pollutants ( $\text{NO}_2$ ,  $\text{O}_3$ ,  $\text{SO}_2$ ,  $\text{PM}_{2.5}$ ,  $\text{PM}_{10}$ ) from the Air Quality e-Reporting database (AQ e-Reporting, <https://www.eea.europa.eu/data-and-maps/data/aqereporting-9>) by European Environmental Agency <https://www.eea.europa.eu>, and measured aerosols from the Aerosol Chemical Speciation Monitor/Aerosol Mass Spectrometer stations. The modeled results were further validated for the year modeled in this study in the supplementary information (particulate matter and its bulk chemical components: Figure SI 8-9).

### 3. Results and discussions

#### 3.1. OA source identification

OA and PM exhibited a strong seasonal variability with maximum concentrations during winter 2013. The  $\text{PM}_{10}$  concentrations that correspond to the days that samples were analysed with the offline AMS approach were similar to the  $\text{PM}_{10}$  concentration distribution of the entire year 2013 (Figure SI 10). In total, we identified six OA components, each with a characteristic chemical composition and temporal behavior, using the offline AMS approach (Fig. 1). POA was represented by four components, and SOA was further separated into two types.

#### 3.2. Primary OA

The Hydrocarbon-like OA (HOA) mass spectral fingerprint was constrained using the HOA profile from Crippa et al. (2013) and was

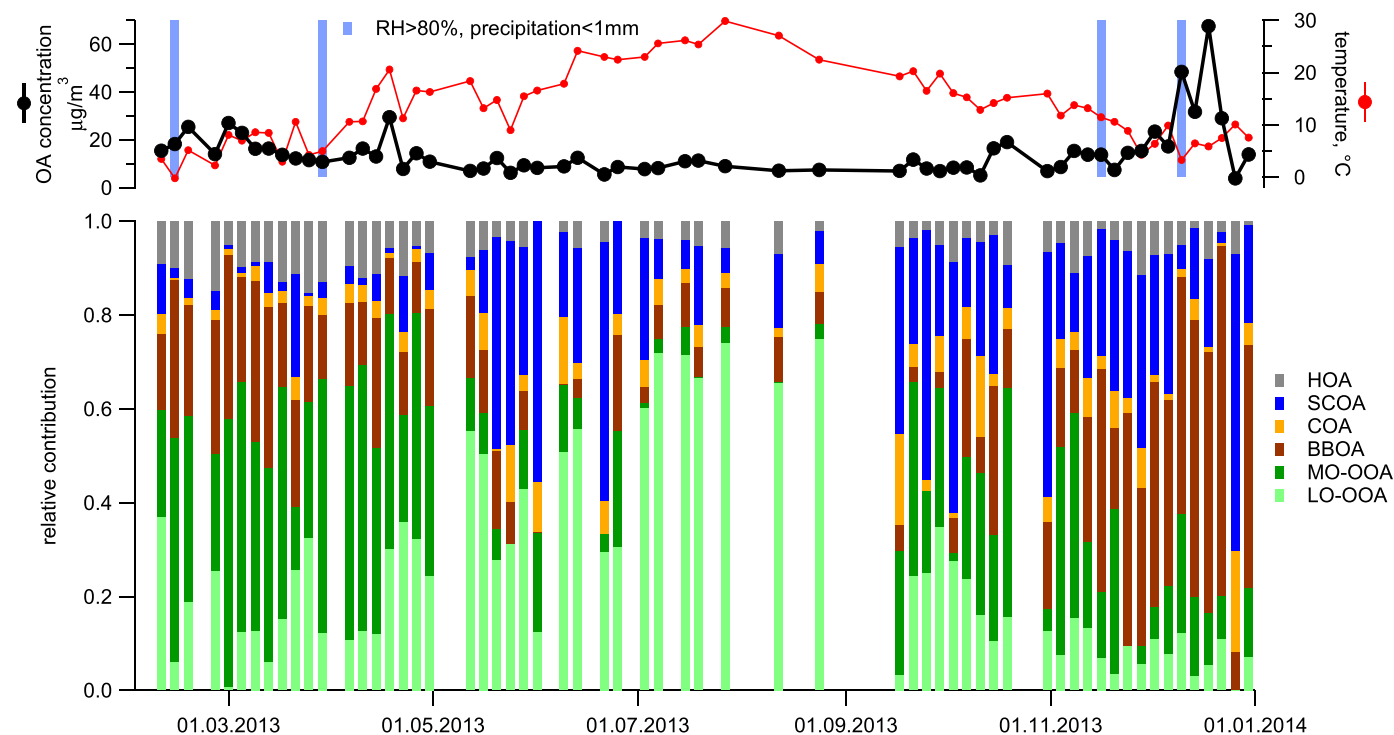


**Fig. 1.** The organic aerosol in Milan and its sources: upper panel: The time series of OA concentrations and daily average temperature. Lower panel: The relative contribution of the different sources to OA in Milan.

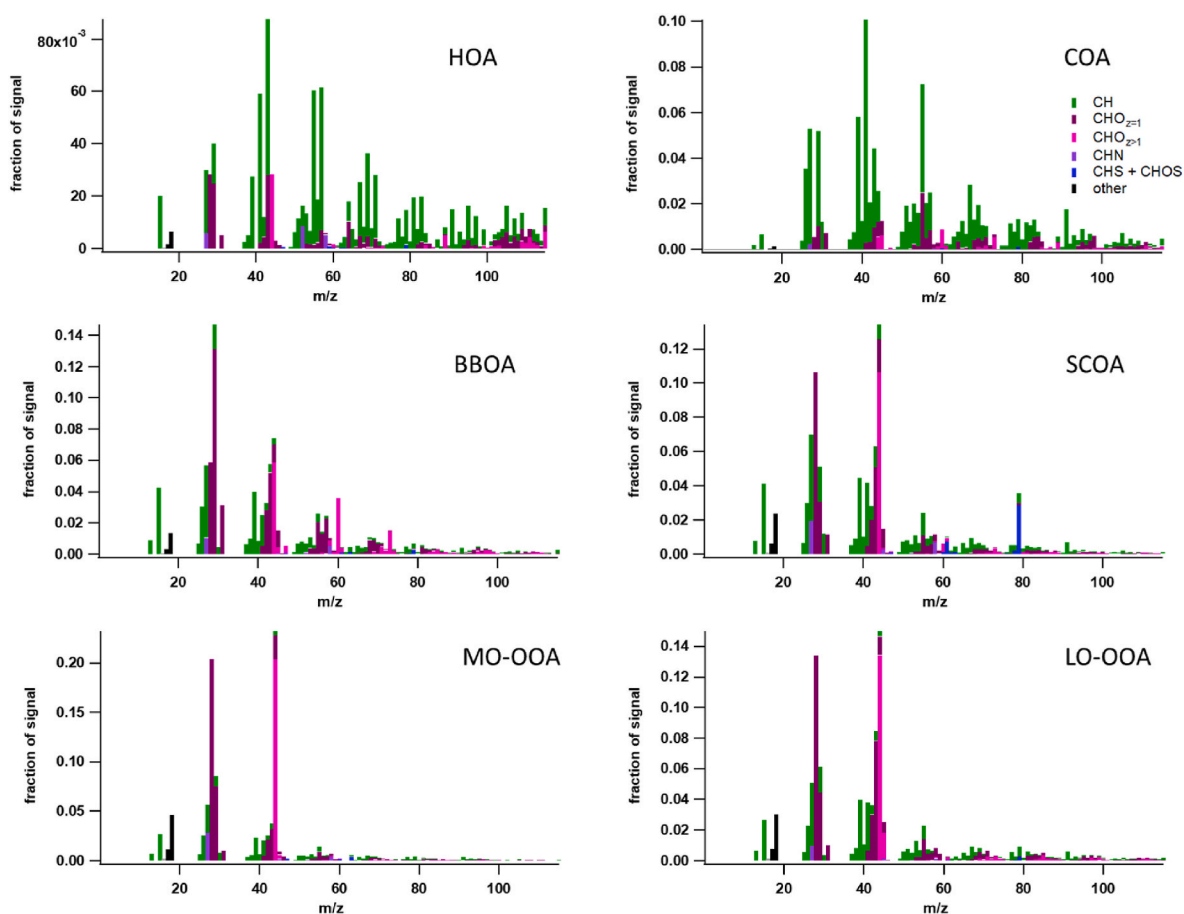


**Fig. 2.** Mass spectral OA fingerprints of OA sources from AMS source apportionment. Fragment ions are grouped in chemical families.



characterized by high contributions of hydrocarbon fragments (OM/OC of 1.29) (Fig. 2). The oxygenated organic fragments at  $m/z > 100$  showed an increased contribution to HOA because they were missing in the original high-resolution reference profile. In consequence, they could only be estimated using the unit mass resolution (UMR) spectra and were assigned an  $a$ -value of unity (see Section 2.3). The concentration time series of HOA showed a similar yearly cycle as traffic emission markers -  $\text{NO}_2$  as well as  $\text{EC}_{\text{traffic}}$  (Fig. 3).  $\text{EC}_{\text{traffic}}$  is the difference between measured EC and EC from biomass burning assuming a ECnon-fossil-to-levoglucosan ratio of 0.87 based on data from southern Swiss alpine valleys (Zotter et al., 2014).

**Sulfur containing OA (SCOA)** showed a prominent contribution of  $\text{CH}_3\text{SO}_2^+$  (explaining 68% of the observed variance of the fragment ion) and is highly oxygenated (OM/OC of 1.93) (Fig. 2). While  $\text{CH}_3\text{SO}_2^+$  is typically regarded as a marker for marine SOA in fine PM, here SCOA in  $\text{PM}_{10}$  did not show a similar temporal variability as methanesulfonic acid – a marker for biogenic marine SOA (Crippa et al., 2013; Zorn et al., 2008; Moschos et al., 2022). This was in line with OA particle types rich in  $\text{CH}_3\text{SO}_2^+$  that were mostly in the coarse mode ( $\text{PM}_{10}>\text{PM}_{2.5}$ ) and largely made of fossil carbon that we found in previous studies (Daellenbach et al., 2017; Vlachou et al., 2018). In addition, these components correlated with vehicular wear identified based on trace metal data in Switzerland (Daellenbach et al., 2020). Overall, it appears likely that here SCOA in  $\text{PM}_{10}$  was related to non-exhaust traffic emissions as suggested in previous studies (Vlachou et al., 2018; Daellenbach et al., 2017, 2020). To further investigate this hypothesis, the SCOA concentration time series was used to constrain a factor in source apportionment analysis using a dataset containing EC, OC, Levoglucosan, metals, and ions. This dataset was previously used in another publication (Amato et al., 2016). Here, we have constrained the analysis using the chemical profiles of all PM sources obtained in Amato et al. (2016) in addition to the SCOA concentration time-series. The goal was to identify the chemical composition of this additional source. The resulting profile contained EC, OC, Al, Si, Ca, Ti, V, Mn, Fe, Ni, Cu, Zn, and  $\text{Mg}^{2+}$  but also sulphate (Figure SI 11). The chemical fingerprint was similar to road dust and tire wear emissions (Thorpe and Harrison, 2008), in line with SCOA being related to non-exhaust traffic emissions. The OC/EC ratio in the factor was  $\sim 12$ , while Cu/Zn is  $\sim 3$ , which are roughly consistent with the values reported in other studies for  $\text{PM}_{10}$  particles related to

road dust emissions in Braga, Portugal (Alves et al., 2018). Previous work suggested that sulfur is present in various non-exhaust traffic particles (tire, brake, road dust) (Amato et al., 2011; Colombi et al., 2011). The potential origin of sulfur is diverse and can be from minerals to vulcanized rubber in tires. The latter could also contribute to  $\text{CH}_3\text{SO}_2^+$  identified by the AMS. However, at this stage the origin of this fragment ion remains unclear.

The **Cooking OA (COA)** mass spectral fingerprint was constrained using the COA profile from Crippa et al. (2013). COA was characterized by a high contribution of hydrocarbon fragments (OM/OC of 1.32) but shows a substantially higher contribution of oxygenated fragment (e.g.  $\text{C}_3\text{H}_3\text{O}^+$ ) than HOA (Fig. 2). For COA, no molecular marker was available for PMF optimization and validation purposes and. Consequentially, COA concentrations were uncertain (Figure SI 7).

**Biomass burning OA (BBOA)** was characterized by high contributions of oxygenated fragments ( $\text{CHO}^+$ ,  $\text{C}_2\text{H}_4\text{O}_2^+$ ,  $\text{C}_3\text{H}_5\text{O}_2^+$ ) from anhydrous sugar fragmentation. Overall the chemical fingerprint of BBOA (OM/OC of 1.74; Fig. 2) was found to be typical for such emissions observed at other locations and similar to the one for levoglucosan (Fig. 3) (Daellenbach et al., 2016; Lanz et al., 2007; Crippa et al., 2013; Alfarrá et al., 2007). The BBOA concentration time series for the study period showed a pronounced seasonal variability with maximum concentrations during winter and correlated with the one of levoglucosan – an anhydrous sugar produced during cellulose pyrolysis. We assumed that BBOA originated from residential heating appliances and not other sources. The main reason was that BBOA as resolved by PMF correlated well with BBOA modeled by CAMx, which only represented residential heating BBOA. (Figure SI 9). Among all OA sources, BBOA correlated strongest with PAHs clearly indicating that BBOA was the major source of PAHs in Milan (Fig. 3).

### 3.3. Secondary OA

Oxygenated OA (OOA) – representing SOA – was separated into a more and a less oxygenated component (*more oxygenated OOA* – MO-OOA: OM/OC of 2.13, *less oxygenated OOA* – LO-OOA: OM/OC of 1.89) (Fig. 2). MO-OOA dominated OOA during winter and correlated well with  $\text{NH}_4^+$  and  $\text{NO}_3^-$ . During the cold period, the Po basin was often foggy. Consequentially, SOA was previously found to be affected by

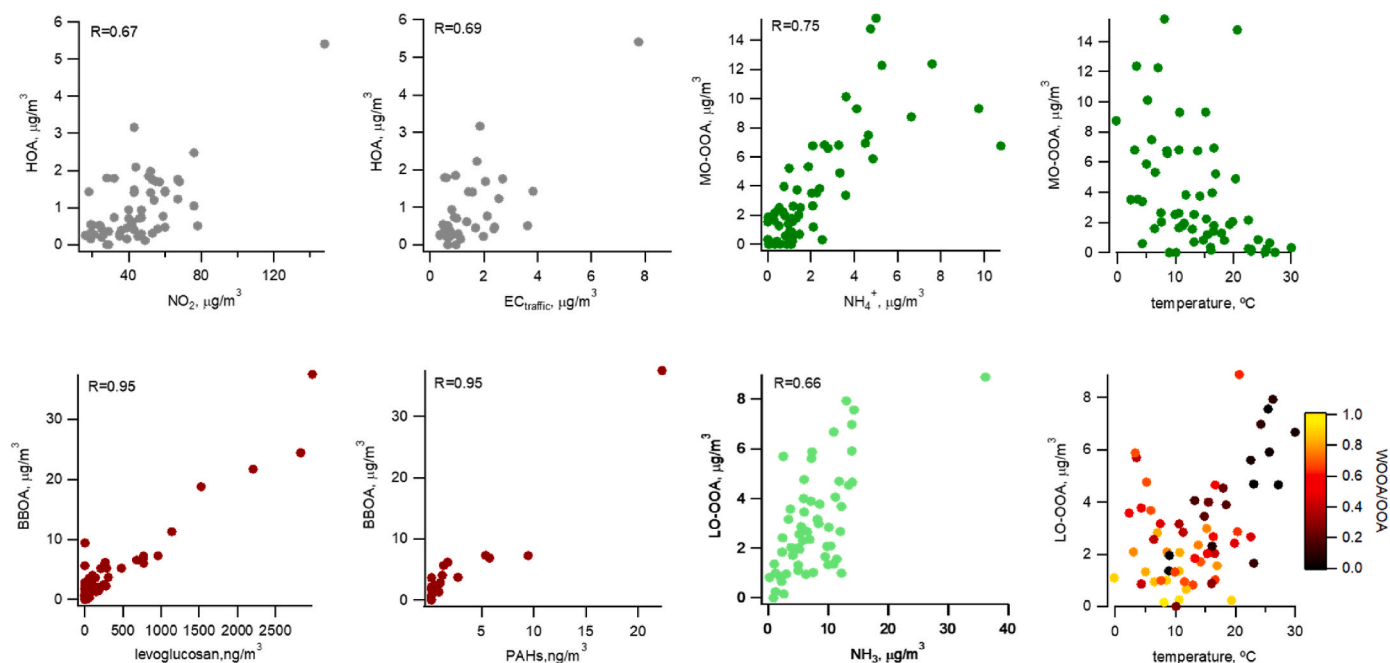


Fig. 3. OA source concentration time series from offline AMS in comparison to chemical and marker concentration time series and other external data.

aqueous processing (Gilardoni et al., 2016; Paglione et al., 2020). Here, neither LO-OOA nor MO-OOA showed a clear relation with the aerosol liquid water content which would be expected for SOA formed via aqueous processes. Still, MO-OOA was enhanced at relative humidities larger than 70% ( $OA_{RH>70}^{source,median}/OA_{RH\leq 70}^{source,median}$ : HOA 1.07, SCOA 0.49, COA 1.06, BBOA 0.91, LO-OOA 0.97, MO-OOA 1.79), suggesting that aqueous chemistry could have contributed to its formation, at least in part.

During summer 2013, LO-OOA dominated SOA, and concentrations increased exponentially, as would be expected for biogenic SOA (Figs. 1 and 3) (Leaitch et al., 2011). However, LO-OOA was also abundant during winter (Fig. 1). Therefore, LO-OOA represented likely rather a mixture of anthropogenic and biogenic SOA during the period of study. In addition, LO-OOA correlated well with gasphase  $NH_3$  ( $R = 0.66$ ) (Fig. 3). This could indicate that 1)  $NH_3$  neutralized acidic organic vapours and thereby drove them into the particle-phase and/or that 2) LO-OOA was formed from SOA precursor emissions occurring from the same source as  $NH_3$ . In addition to a clear influence of emissions from the Po basin on OOA, air mass back trajectory analyses (Figure SI 12) showed that air parcels characterized with high LO-OOA concentrations spent substantial amounts of time over e.g. southeastern Germany where high biogenic SOA concentrations are expected (Jiang et al., 2019). Based on these results, it remains uncertain what sources and processes govern SOA in Milan overall.

### 3.4. Contribution to SOA by different emission sectors

We further investigated the sources of SOA by combining the offline AMS source apportionment with air quality modelling results. The air quality modelling results from CAMx were largely in line with the field observations and source apportionment results (particulate matter and its bulk chemical components: Figure SI 8-9). At other locations (e.g. Zurich) where biogenic emissions dominated SOA in summer, seasonally separated SOA from offline AMS analyses could be related to biogenic SOA and anthropogenic – largely residential biomass burning – SOA (Daellenbach et al., 2017, 2020, 2019; Qi et al., 2020). Here, for Milan, SOA found by offline AMS analyses was split into two components (LO-OOA and MO-OOA) with different seasonality without a clear relation to its emission sources. We found that MO-OOA correlated well with the biomass burning SOA from CAMx ( $R = 0.74$ , Fig. 4). This suggested that MO-OOA is related to biomass burning SOA. LO-OOA, on the other hand, correlated well with the sum of all other anthropogenic (traffic + other anthropogenic – industry, energy production, shipping-sectors) and biogenic SOA ( $R = 0.63$ , Fig. 4) – better with the anthropogenic ( $R_{Pr,trafficSOA} = 0.67$ ,  $R_{Pr,otheranthroSOA} = 0.58$ ) than with the biogenic fraction ( $R_{Pr,bioSOA} = 0.50$ ). Thus, LO-OOA was likely a mixture of anthropogenic and biogenic SOA.

### 3.5. Sources contribution to OA

During the cold period (Oct–Mar 2013), POA contributed 62% to OA, with the largest contribution from BBOA (37%). During the warm period (Apr–Sep), POA contributed less to OA (38%). This decrease was largely related to the lower BBOA concentrations, while other POA contributed similarly to OA (Fig. 5). In terms of OC, these results were in line with previous work for winter but also showed discrepancies in summer (Figure SI 13) (Amato et al., 2016). Both approaches found that POC (Amato et al., 2016): vehicle exhaust, vehicle non-exhaust, biomass burning, mineral dust, this study: HOA, SCOA, COA, BBOA) – with a dominant fraction from residential biomass burning emissions – was more important in winter than in summer. While both approaches found OC related to exhaust and non-exhaust traffic POC, the exact splits differ, and Amato et al., 2016 found an additional contribution from mineral dust.

We found that SOA was the main contributor to OA and also responsible for high OA episodes during the warm period, while high OA levels during the cold period were strongly related to BBOA for the period of study (Fig. 5). The important role of BBOA for OA pollution episodes in winter was in line with a large contribution of non-fossil fuels to OC during winter (Bernardoni et al., 2013). In addition to OA, residential heating biomass burning emissions also contained inorganic components such as potassium ( $K^+$ ). Here, we observed relatively high BBOA-to- $K^+$  ratios (BBOA-to- $K^+$  19.4) which were similar to observations from alpine valleys in southern Switzerland (BBOA-to- $K^+$  18.1) but distinctly higher than in the Swiss Plateau north of the Alps (BBOA-to- $K^+$  3.4) (Fig. 6). In a previous study, the enhanced BBOA-to- $K^+$  were related to inefficient residential combustion conditions in the alpine valleys (Daellenbach et al., 2018). The comparable BBOA-to- $K^+$  ratios in Milano suggested that the large contribution of BBOA to OA were to a large extent, caused by similarly inefficient combustion conditions in residential heating appliances. Based on levoglucosan analyses, we estimated BBOA concentrations for the period 2012–2022 (BBOA-to-levoglucosan ratio 12, Fig. 6). Both the BBOA-to- $K^+$  ratio (varied from year to year between 11 and 23, for each year: Jan–Mar + Oct–Dec for days with levoglucosan  $>0.05 \mu g/m^3$ ) as well as the BBOA concentrations remained approximately constant. Thus, emissions from inefficient residential heating biomass burning could be expected to still be the major driver of winter-time OA pollution in Milan. Yet, the contribution of other OA sources – especially SOA – might have changed and will need to be quantified in future research.

## 4. Conclusions

The Milan metropolitan area in the Po basin in northern Italy is a European air pollution hotspot and experienced severe particulate matter pollution episodes historically – mostly in winter – with a high

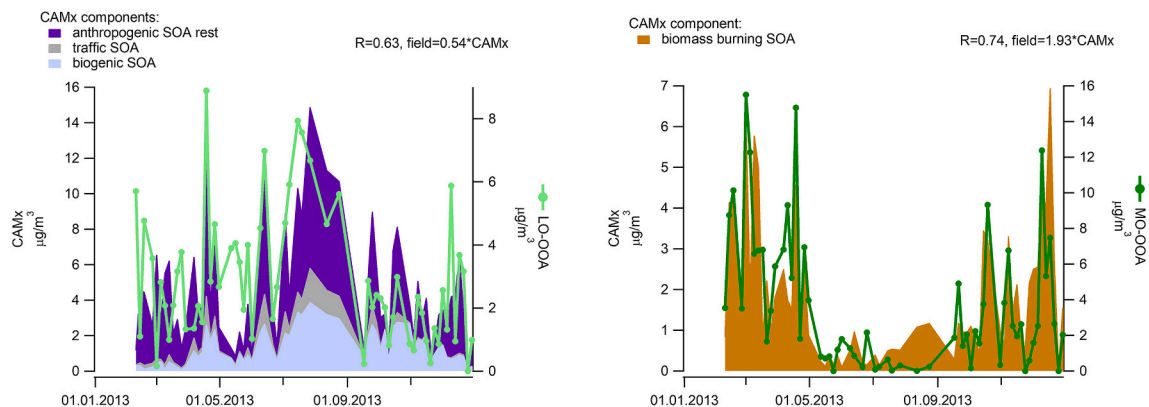
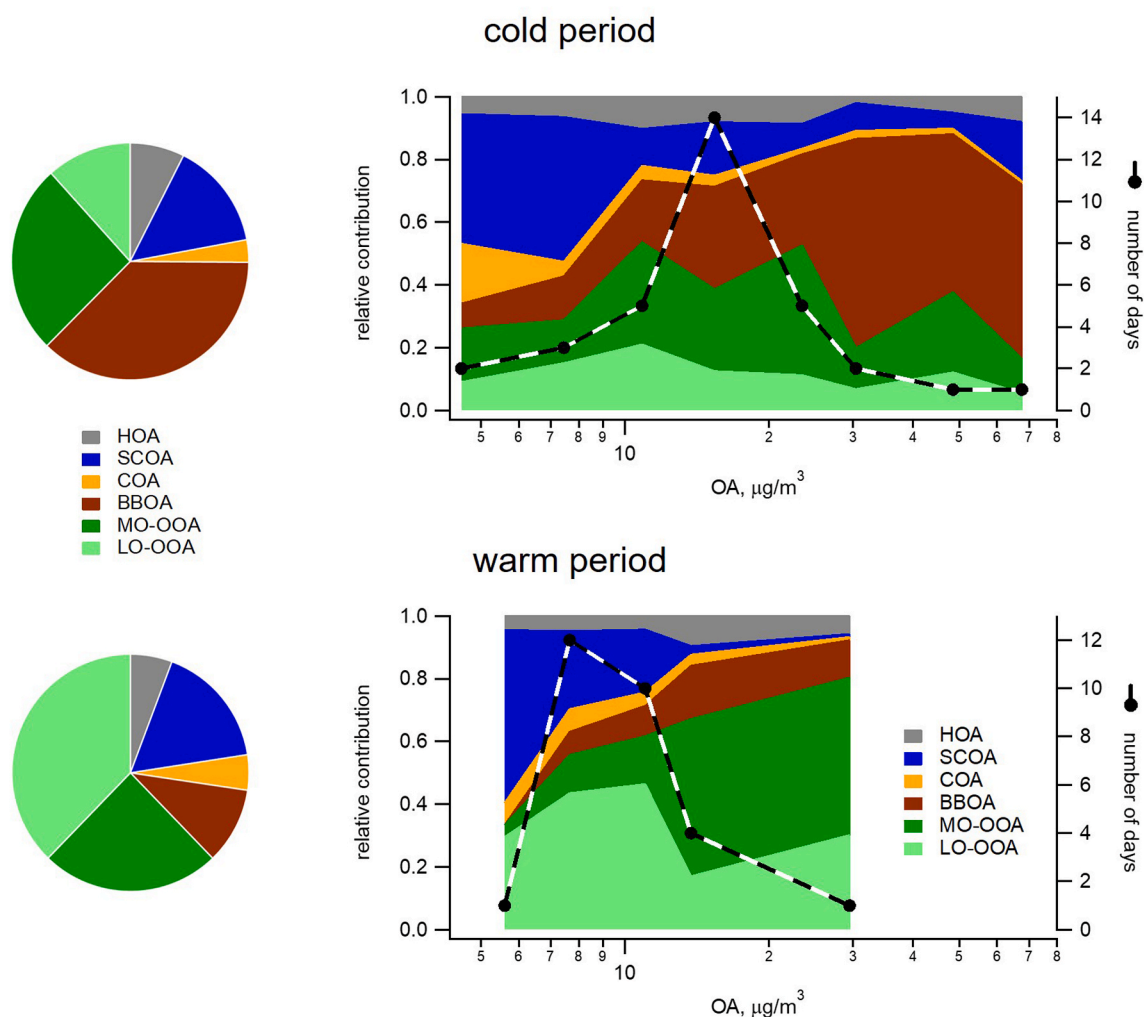
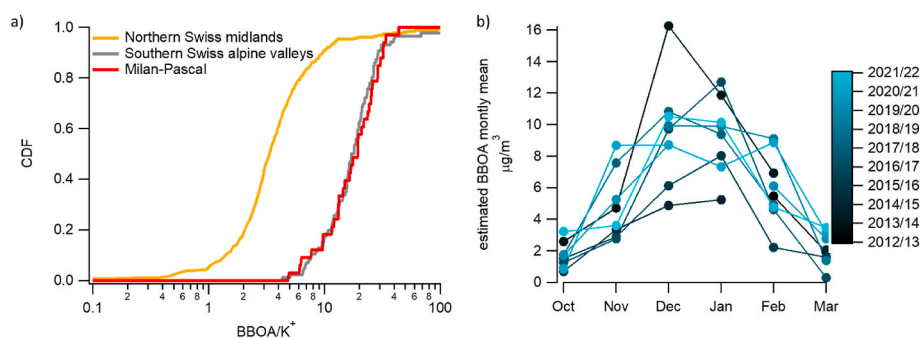


Fig. 4. Comparison of offline AMS OOA (LO-OOA and MO-OOA) and SOA sources from the air quality model CAMx.



**Fig. 5.** Relative contribution of OA sources during the cold (Oct–Mar, HOA: 7%, SCOA: 15%, COA: 3%, BBOA: 37%, MO-OOA: 26%, LO-OOA: 12%) and warm season (Apr–Sep, HOA: 6%, SCOA: 17%, COA: 5%, BBOA: 10%, MO-OOA: 24%, LO-OOA: 38%). OA sources are displayed for the cold (Oct–Mar) warm period (Apr–Sep) as mean relative contributions and as a function of OA concentrations.



**Fig. 6.** a) Cumulative distribution functions (CDF) of BBOA-to- $K^+$  concentration ratios for the Northern Swiss midlands, southern Swiss alpine valleys, and Milan-Pascal (all PM10) during the cold period (Oct–Mar) for 2013, b) evolution of monthly mean estimated BBOA concentrations (12 times the concentration of levoglucosan) between 2012 and 2022.

contribution of OA from largely unknown sources. In this study, we quantified for the first time the sources of OA in Milan based on the year 2013. We found, that during the period of study, residential heating biomass burning POA (BBOA) governed OA in Milan during winter, especially during polluted conditions. Such emissions further controlled the levels of carcinogenic PAHs. Inefficient combustion conditions identified by high BBOA/ $K^+$  ratios contributed to the high relative

contribution of BBOA to OA. We found that emissions from inefficient residential heating biomass burning were still (2012–2022) a major driver of winter-time OA pollution in Milan, yet assessing changes in the contribution of other OA sources requires future research. While POA (HOA + SCOA + COA + BBOA) was a most important contributor to OA during winter 2013, SOA dominated OA during summer 2013 – here distinguished by degree of oxygenation (LO-OOA, MO-OOA).



Combining offline AMS source apportionment with air quality modelling results, we found that SOA from residential heating biomass burning emissions was a major contributor to winter-time SOA, while summer-time SOA was a mixture formed from both biogenic and anthropogenic emissions (traffic, industry, energy production, shipping) during the study period. The results provide a baseline for comparison to the present situation, which is necessary for implementing and assessing mitigation policies. As the sources that affect SOA are largely unknown on a global scale, this study can be used as an example methodology for combining OA source apportionment analyses based on chemical analyses with bottom-up air quality OA source analyses to understand the formation of SOA better.

## Contribution statement

Kaspar R. Daellenbach: Conception and design of study, acquisition of data, analysis and/or interpretation of data, writing - original draft, visualization, Manousos Manousakas: analysis and/or interpretation of data, Writing - Original Draft, Jianhui Jiang: acquisition of data, writing - review/editing, Tianqu Cui: analysis and/or interpretation of data, writing - review/editing, Ying Chen: acquisition of data, writing - review/editing, Imad El Haddad: acquisition of data, analysis and/or interpretation of data, writing - review/editing, Paola Fermo: acquisition of data, writing - review/editing, Cristina Colombi: acquisition of data, writing - review/editing, A. S. H. Prévôt: analysis and/or interpretation of data, writing - review/editing.

## Declaration of competing interest

The authors declare the following financial interests/personal relationships which may be considered as potential competing interests: Kaspar R. Daellenbach reports financial support was provided by Swiss National Science Foundation.

## Data availability

The dataset shown in the figures is publicly available at [10.5281/zenodo.7937473](https://doi.org/10.5281/zenodo.7937473).

## Acknowledgements

K.R.D. acknowledges support by the Swiss National Science Foundation Ambizione grant PZPGP2.201992. We acknowledge Giulia Stefanelli for support in the offline AMS analyses and Jean-Luc Jaffrezzo for WSOC analyses. We like to thank the Swiss Federal Office of the Environment (FOEN) and the Swiss Data Science Centre (SDSC, AURORA project) for their financial support for the aerosol modelling.

## Appendix A. Supplementary data

Supplementary data to this article can be found online at <https://doi.org/10.1016/j.atmosenv.2023.119799>.

## References

- Alfarra, M.R., Prevot, A.S.H., Szidat, S., Sandradewi, J., Weimer, S., Lanz, V.A., Schreiber, D., Mohr, M., Baltensperger, U., 2007. Identification of the mass spectral signature of organic aerosols from wood burning emissions. *Environ. Sci. Technol.* 41, 5770–5777. <https://doi.org/10.1021/es062289b>.
- Alves, C.A., Evtugina, M., Vicente, A.M.P., Vicente, E.D., Nunes, T.V., Silva, P.M.A., Duarte, M.A.C., Pio, C.A., Amato, F., Querol, X., 2018. Chemical profiling of PM10 from urban road dust. *Sci. Total Environ.* 634, 41–51. <https://doi.org/10.1016/j.scitotenv.2018.03.338>.
- Amato, F., Pandolfi, M., Moreno, T., Furger, M., Pey, J., Alastuey, A., Bukowiecki, N., Prevot, A.S.H., Baltensperger, U., Querol, X., 2011. Sources and variability of inhalable road dust particles in three European cities. *Atmos. Environ.* 45, 6777–6787. <https://doi.org/10.1016/j.atmosenv.2011.06.003>.
- Amato, F., Alastuey, A., Karanasiou, A., Lucarelli, F., Nava, S., Calzolari, G., Severi, M., Becagli, S., Gianelle, V.L., Colombi, C., Alves, C., Custódio, D., Nunes, T., Cerqueira, M., Pio, C., Eleftheriadis, K., Diapouli, E., Reche, C., Minguillón, M.C., Manousakas, M.I., Maggos, T., Vratolis, S., Harrison, R.M., Querol, X., 2016. AIRUSE-LIFE+: a harmonized PM speciation and source apportionment in five southern European cities. *Atmos. Chem. Phys.* 16, 3289–3309. <https://doi.org/10.5194/acp-16-3289-2016>.
- Bates, J.T., Fang, T., Verma, V., Zeng, L., Weber, R.J., Tolbert, P.E., Abrams, J.Y., Sarnat, S.E., Klein, M., Mulholland, J.A., Russell, A.G., 2019. Review of acellular assays of ambient particulate matter oxidative potential: methods and relationships with composition, sources, and health effects. *Environ. Sci. Technol.* 53, 4003–4019. <https://doi.org/10.1021/acs.est.8b03430>.
- Bernardini, V., Calzolari, G., Chiari, M., Fedi, M., Lucarelli, F., Nava, S., Piazzalunga, A., Riccobono, F., Taccetti, F., Valli, G., Vecchi, R., 2013. Radiocarbon analysis on organic and elemental carbon in aerosol samples and source apportionment at an urban site in Northern Italy. *J. Aerosol Sci.* 56, 88–99. <https://doi.org/10.1016/j.jaerosci.2012.06.001>.
- Bhandari, S., Arub, Z., Habib, G., Apte, J.S., Hildebrandt Ruiz, L., 2022. Contributions of primary sources to submicron organic aerosols in Delhi, India. *Atmos. Chem. Phys.* 22, 13631–13657. <https://doi.org/10.5194/acp-22-13631-2022>.
- Birch, M.E., Cary, R.A., 1996. Elemental carbon-based method for monitoring occupational exposures to particulate diesel exhaust. *Aerosol Sci. Tech.* 25, 221–241. <https://doi.org/10.1080/02786829608965393>.
- Bozzetti, C., El Haddad, I., Salameh, D., Daellenbach, K.R., Fermo, P., Gonzalez, R., Minguillón, M.C., Iinuma, Y., Poulain, L., Elser, M., Müller, E., Slowik, J.G., Jaffrezzo, J.L., Baltensperger, U., Marchand, N., Prévôt, A.S.H., 2017a. Organic aerosol source apportionment by offline-AMS over a full year in Marseille. *Atmos. Chem. Phys.* 17, 8247–8268. <https://doi.org/10.5194/acp-17-8247-2017>.
- Bozzetti, C., Sosedova, Y., Xiao, M., Daellenbach, K.R., Ulevicius, V., Dudoitis, V., Mordas, G., Byčenkienė, S., Plauskaitė, K., Vlachou, A., Golly, B., Chazneau, B., Besombes, J.L., Baltensperger, U., Jaffrezzo, J.L., Slowik, J.G., El Haddad, I., Prévôt, A.S.H., 2017b. Argon offline-AMS source apportionment of organic aerosol over yearly cycles for an urban, rural, and marine site in northern Europe. *Atmos. Chem. Phys.* 17, 117–141. <https://doi.org/10.5194/acp-17-117-2017>.
- Bozzetti, C., Daellenbach, K.R., Hueglin, C., Fermo, P., Sciare, J., Kasper-Giebl, A., Mazur, Y., Abbaszade, G., El Kazzi, M., Gonzalez, R., Shuster-Meiseles, T., Flasch, M., Wolf, R., Krepelová, A., Canonaco, F., Schnelle-Kreis, J., Slowik, J.G., Zimmermann, R., Rudich, Y., Baltensperger, U., El Haddad, I., Prévôt, A.S.H., 2016. Size-resolved identification, characterization, and quantification of primary biological organic aerosol at a European rural site. *Environ. Sci. Technol.* 50, 3425–3434. <https://doi.org/10.1021/acs.est.5b05960>.
- Bressi, M., Cavalli, F., Belis, C.A., Putaud, J.P., Fröhlich, R., Martins dos Santos, S., Petralia, E., Prévôt, A.S.H., Berico, M., Malaguti, A., Canonaco, F., 2016. Variations in the chemical composition of the submicron aerosol and in the sources of the organic fraction at a regional background site of the Po Valley (Italy). *Atmos. Chem. Phys.* 16, 12875–12896. <https://doi.org/10.5194/acp-16-12875-2016>.
- Bressi, M., Cavalli, F., Putaud, J.P., Fröhlich, R., Petit, J.E., Aas, W., Aijälä, M., Alastuey, A., Allan, J.D., Aurela, M., Berico, M., Bougiatioti, A., Bukowiecki, N., Canonaco, F., Crenn, V., Dusanter, S., Ehn, M., Elsasser, M., Flentje, H., Graf, P., Green, D.C., Heikkinen, L., Hermann, H., Holzinger, R., Hueglin, C., Keernik, H., Kiendler-Scharr, A., Kubelová, L., Lunder, C., Maasikmet, M., Makeš, O., Malaguti, A., Mihalopoulos, N., Nicolas, J.B., O'Dowd, C., Ovadnevaite, J., Petralia, E., Poulain, L., Priestman, M., Riffault, V., Ripoll, A., Schlag, P., Schwarz, J., Sciare, J., Slowik, J., Sosedova, Y., Stavroulas, I., Teinmaa, E., Via, M., Vodička, P., Williams, P.I., Wiedensohler, A., Young, D.E., Zhang, S., Favez, O., Minguillón, M.C., Prevot, A.S.H., 2021. A European aerosol phenomenology - 7: high-time resolution chemical characteristics of submicron particulate matter across Europe. *Atmos. Environ.* X 10, 100108. <https://doi.org/10.1016/j.aeaoa.2021.100108>.
- Canagaratna, M.R., Jayne, J.T., Jimenez, J.L., Allan, J.D., Alfarra, M.R., Zhang, Q., Onasch, T.B., Drewnick, F., Coe, H., Middlebrook, A., Delia, A., Williams, L.R., Trimborn, A.M., Northway, M.J., DeCarlo, P.F., Kolb, C.E., Davidovits, P., Worsnop, D.R., 2007. Chemical and microphysical characterization of ambient aerosols with the aerodyne aerosol mass spectrometer. *Mass Spectrom. Rev.* 26, 185–222. <https://doi.org/10.1002/mas.20115>.
- Canonaco, F., Crippa, M., Slowik, J.G., Baltensperger, U., Prévôt, A.S.H., 2013. SoFi, an IGOR-based interface for the efficient use of the generalized multilinear engine (ME-2) for the source apportionment: ME-2 application to aerosol mass spectrometer data. *Atmos. Meas. Tech.* 6, 3649–3661. <https://doi.org/10.5194/amt-6-3649-2013>.
- Canonaco, F., Tobler, A., Chen, G., Sosedova, Y., Slowik, J.G., Bozzetti, C., Daellenbach, K.R., El Haddad, I., Crippa, M., Huang, R.J., Furger, M., Baltensperger, U., Prévôt, A.S.H., 2021. A new method for long-term source apportionment with time-dependent factor profiles and uncertainty assessment using SoFi Pro: application to 1 year of organic aerosol data. *Atmos. Meas. Tech.* 14, 923–943. <https://doi.org/10.5194/amt-14-923-2021>.
- Casotto, R., Cvitešić Kušan, A., Bhattu, D., Cui, T., Manousakas, M.I., Frka, S., Kroflič, A., Grčić, I., Ciglenečki, I., Baltensperger, U., Slowik, J.G., Daellenbach, K.R., Prévôt, A.S.H., 2022a. Chemical composition and sources of organic aerosol on the Adriatic coast in Croatia. *Atmos. Environ.* X 13, 100159. <https://doi.org/10.1016/j.aeaoa.2022.100159>.
- Casotto, R., Skiba, A., Rauber, M., Strähl, J., Tobler, A., Bhattu, D., Lamkaddam, H., Manousakas, M.I., Salazar, G., Cui, T., Canonaco, F., Samek, L., Ryš, A., El Haddad, I., Kasper-Giebl, A., Baltensperger, U., Necki, J., Szidat, S., Styszko, K., Slowik, J.G., Prévôt, A.S.H., Daellenbach, K.R., 2022b. Organic aerosol sources in Krakow, Poland, before implementation of a solid fuel residential heating ban. *Sci. Total Environ.*, 158655. <https://doi.org/10.1016/j.scitotenv.2022.158655>.
- Chen, G., Canonaco, F., Tobler, A., Aas, W., Alastuey, A., Allan, J., Atabakhsh, S., Aurela, M., Baltensperger, U., Bougiatioti, A., De Brito, J.F., Ceburnis, D., Chazneau, B., Chebaicheb, H., Daellenbach, K.R., Ehn, M., El Haddad, I.,



- Eleftheriadis, K., Favez, O., Flentje, H., Font, A., Fossum, K., Freney, E., Gini, M., Green, D.C., Heikkinen, L., Herrmann, H., Kalogridis, A.-C., Keernik, H., Lhotka, R., Lin, C., Lunder, C., Maasilkmet, M., Manousakas, M.I., Marchand, N., Marin, C., Marmureanu, L., Mihalopoulos, N., Močnik, G., Nećki, J., O'Dowd, C., Ovadnevaite, J., Peter, T., Petit, J.-E., Pikridas, M., Matthew Platt, S., Pokorná, P., Poulain, L., Priestman, M., Riffault, V., Rinaldi, M., Różański, K., Schwarz, J., Sciare, J., Simon, L., Skiba, A., Slowik, J.G., Sosodova, Y., Stavroulas, I., Styszko, K., Teinmaa, E., Timonen, H., Tremper, A., Vasilescu, J., Via, M., Vodička, P., Wiedensohler, A., Zografou, O., Cruz Mingüillón, M., Prévôt, A.S.H., 2022. European aerosol phenomenology – 8: harmonised source apportionment of organic aerosol using 22 Year-long ACSM/AMS datasets. *Environ. Int.* 166, 107325 <https://doi.org/10.1016/j.envint.2022.107325>.
- Chen, Y., Takeuchi, M., Nah, T., Xu, L., Canagaratna, M.R., Stark, H., Baumann, K., Canonaco, F., Prévôt, A.S.H., Huey, L.G., Weber, R.J., Ng, N.L., 2020. Chemical characterization of secondary organic aerosol at a rural site in the southeastern US: insights from simultaneous high-resolution time-of-flight aerosol mass spectrometer (HR-ToF-AMS) and FIGAERO chemical ionization mass spectrometer (CIMS) measurements. *Atmos. Chem. Phys.* 20, 8421–8440. <https://doi.org/10.5194/acp-20-8421-2020>.
- Colombi, C., Gianelle, V.L., Belis, C., Larsen, B.R., 2011. Determination of local source profile for soil dust, brake dust and biomass burning sources. *Chem. Eng. Trans.* <https://doi.org/10.3303/CET1022038>.
- Crippa, M., El Haddad, I., Slowik, J.G., DeCarlo, P.F., Mohr, C., Hering, M.F., Chirico, R., Marchand, N., Sciare, J., Baltensperger, U., Prévôt, A.S.H., 2013. Identification of marine and continental aerosol sources in Paris using high resolution aerosol mass spectrometry. *J. Geophys. Res. Atmos.* 118, 1950–1963. <https://doi.org/10.1002/jgrd.50151>.
- Daellenbach, K.R., Uzu, G., Jiang, J., Cassagnes, L.-E., Leni, Z., Vlachou, A., Stefanelli, G., Canonaco, F., Weber, S., Segers, A., 2020. Sources of particulate-matter air pollution and its oxidative potential in Europe. *Nature* 587, 414–419. <https://doi.org/10.1038/s41586-020-2902-8>.
- Daellenbach, K.R., Kourtev, I., Vogel, A.L., Bruns, E.A., Jiang, J., Petäjä, T., Jaffrezo, J. L., Aksoyoglu, S., Kalberer, M., Baltensperger, U., El Haddad, I., Prévôt, A.S.H., 2019. Impact of anthropogenic and biogenic sources on the seasonal variation in the molecular composition of urban organic aerosols: a field and laboratory study using ultra-high-resolution mass spectrometry. *Atmos. Chem. Phys.* 19, 5973–5991. <https://doi.org/10.5194/acp-19-5973-2019>.
- Daellenbach, K.R., Bozzetti, C., Krepešlová, A., Canonaco, F., Wolf, R., Zotter, P., Fermo, P., Crippa, M., Slowik, J.G., Sosodova, Y., Zhang, Y., Huang, R.J., Poulain, L., Szidat, S., Baltensperger, U., El Haddad, I., Prévôt, A.S.H., 2016. Characterization and source apportionment of organic aerosol using offline aerosol mass spectrometry. *Atmos. Meas. Tech.* 9, 23–39. <https://doi.org/10.5194/amt-9-23-2016>.
- Daellenbach, K.R., Stefanelli, G., Bozzetti, C., Vlachou, A., Fermo, P., Gonzalez, R., Piazzalunga, A., Colombi, C., Canonaco, F., Hueglin, C., Kasper-Giebl, A., Jaffrezo, J. L., Bianchi, F., Slowik, J.G., Baltensperger, U., El-Haddad, I., Prévôt, A.S.H., 2017. Long-term chemical analysis and organic aerosol source apportionment at nine sites in central Europe: source identification and uncertainty assessment. *Atmos. Chem. Phys.* 17, 13265–13282. <https://doi.org/10.5194/acp-17-13265-2017>.
- Daellenbach, K.R., El-Haddad, I., Karvonen, L., Vlachou, A., Corbin, J.C., Slowik, J.G., Hering, M.F., Bruns, E.A., Luedin, S.M., Jaffrezo, J.L., Szidat, S., Piazzalunga, A., Gonzalez, R., Fermo, P., Plüger, V., Vogel, G., Baltensperger, U., Prévôt, A.S.H., 2018. Insights into organic-aerosol sources via a novel laser-desorption/ionization mass spectrometry technique applied to one year of PM10 samples from nine sites in central Europe. *Atmos. Chem. Phys.* 18, 2155–2174. <https://doi.org/10.5194/acp-18-2155-2018>.
- EEA, 2016. European environment agency air quality in Europe 2016. Report No. 28/2016. <https://www.eea.europa.eu/publications/air-quality-in-europe-2016>.
- European Committee for Standardization (CEN), 2008. EN 15549:2008 – air quality – standard method for the measurement of the concentration of benzo[a]pyrene in air. CEN.
- Gao, D., Ripley, S., Weichenthal, S., Godri Pollitt, K.J., 2020. Ambient particulate matter oxidative potential: chemical determinants, associated health effects, and strategies for risk management. *Free Radic. Biol. Med.* 151, 7–25. <https://doi.org/10.1016/j.freeradbiomed.2020.04.028>.
- Giannoni, M., Calzolari, G., Chiari, M., Lucarelli, F., Mazzinghi, A., Nava, S., Ruberto, C., 2015. Feasibility study of ED-XRF analysis of atmospheric particulate matter samples collected with high time resolution. *X Ray Spectrom.* 44, 282–288. <https://doi.org/10.1002/xrs.2620>.
- Gilardoni, S., Massoli, P., Paglione, M., Giulianelli, L., Carbone, C., Rinaldi, M., Decesari, S., Sandrini, S., Costabile, F., Gobbi, G.P., Pietrogro, M.C., Visentin, M., Scotto, F., Fuzzi, S., Facchini, M.C., 2016. Direct observation of aqueous secondary organic aerosol from biomass-burning emissions. *Proc. Natl. Acad. Sci. USA* 113, 10013–10018. <https://doi.org/10.1073/pnas.1602212113>.
- Hallquist, M., Wenger, J.C., Baltensperger, U., Rudich, Y., Simpson, D., Claeys, M., Dommen, J., Donahue, N.M., George, C., Goldstein, A.H., Hamilton, J.F., Herrmann, H., Hoffmann, T., Iinuma, Y., Jang, M., Jenkin, M.E., Jimenez, J.L., Kiendler-Scharr, A., Maenhaut, W., McFiggans, G., Mentel, T.F., Monod, A., Prévôt, A.S.H., Seinfeld, J.H., Surratt, J.D., Szmigielski, R., Wildt, J., 2009. The formation, properties and impact of secondary organic aerosol: current and emerging issues. *Atmos. Chem. Phys.* 9, 5155–5236. <https://doi.org/10.5194/acp-9-5155-2009>.
- Henry, R.C., Hidy, G.M., 1979. Multivariate analysis of particulate sulfate and other air quality variables by principal components Part I: annual data from Los Angeles and New York. *Atmos. Environ. Times* 13, 1581–1596. [https://doi.org/10.1016/0004-6981\(79\)90068-4](https://doi.org/10.1016/0004-6981(79)90068-4).
- Hopke, P.K., 2003. Recent developments in receptor modeling. *J. Chemom.* 17, 255–265. <https://doi.org/10.1002/cem.796>.
- Huang, R.-J., Zhang, Y., Bozzetti, C., Ho, K.-F., Cao, J.-J., Han, Y., Daellenbach, K.R., Slowik, J.G., Platt, S.M., Canonaco, F., Zotter, P., Wolf, R., Pieber, S.M., Bruns, E.A., Crippa, M., Ciarelli, G., Piazzalunga, A., Schikowski, M., Abbaszade, G., Schnelle-Kreis, J., Zimmermann, R., An, Z., Szidat, S., Baltensperger, U., Haddad, I.E., Prévôt, A.S.H., 2014. High secondary aerosol contribution to particulate pollution during haze events in China. *Nature* 514, 218–222. <https://doi.org/10.1038/nature13774>.
- Jaffrezo, J.L., Calas, N., Bouchet, M., 1998. Carboxylic acids measurements with ionic chromatography. *Atmos. Environ.* 32, 2705–2708. [https://doi.org/10.1016/S1352-2310\(98\)00026-0](https://doi.org/10.1016/S1352-2310(98)00026-0).
- Jiang, J., El Haddad, I., Aksoyoglu, S., Stefanelli, G., Bertrand, A., Marchand, N., Canonaco, F., Petit, J.E., Favez, O., Gilardoni, S., Baltensperger, U., Prévôt, A.S.H., 2021. Influence of biomass burning vapor wall loss correction on modeling organic aerosols in Europe by CAMx v6.50. *Geosci. Model Dev* 14, 1681–1697. <https://doi.org/10.5194/gmd-14-1681-2021>.
- Jiang, J., Aksoyoglu, S., El-Haddad, I., Ciarelli, G., Denier van der Gon, H.A.C., Canonaco, F., Gilardoni, S., Paglione, M., Mingüillón, M.C., Favez, O., Zhang, Y., Marchand, N., Hao, L., Virtanen, A., Florou, K., O'Dowd, C., Ovadnevaite, J., Baltensperger, U., Prévôt, A.S.H., 2019. Sources of organic aerosols in Europe: a modeling study using CAMx with modified volatility basis set scheme. *Atmos. Chem. Phys.* 19, 15247–15270. <https://doi.org/10.5194/acp-19-15247-2019>.
- Jimenez, J.L., Canagaratna, M.R., Donahue, N.M., Prévôt, A.S.H., Zhang, Q., Kroll, J.H., DeCarlo, P.F., Allan, J.D., Coe, H., Ng, N.L., Aiken, A.C., Docherty, K.S., Ulbrich, I. M., Grieshop, A.P., Robinson, A.L., Duplissy, J., Smith, J.D., Wilson, K.R., Lanz, V.A., Hueglin, C., Sun, Y.L., Tian, J., Laaksonen, A., Raatikainen, T., Rautiainen, J., Vaattovaara, P., Ehn, M., Kulmala, M., Tomlinson, J.M., Collins, D.R., Cubison, M.J., Dunlea, E.J., Huffman, J.A., Onasch, T.B., Alfarra, M.R., Williams, P.I., Bower, K., Kondo, Y., Schneider, J., Drewnick, F., Borrmann, S., Weimer, S., Demerjian, K., Salcedo, D., Cottrell, L., Griffin, R., Takami, A., Miyoshi, T., Hatakeyama, S., Shimono, A., Sun, J.Y., Zhang, Y.M., Dzepina, K., Kimmel, J.R., Sueper, D., Jayne, J. T., Herndon, S.C., Trimborn, A.M., Williams, L.R., Wood, E.C., Middlebrook, A.M., Kolb, C.E., Baltensperger, U., Worsnop, D.R., 2009. Evolution of organic aerosols in the atmosphere. *Science* 326, 1525–1529. <https://doi.org/10.1126/science.1180353>.
- Kuenen, J., Dellaert, S., Visschedijk, A., Jalkanen, J.P., Super, I., Denier van der Gon, H., 2022. CAMS-REG-v4: a state-of-the-art high-resolution European emission inventory for air quality modelling. *Earth Syst. Sci. Data* 14, 491–515. <https://doi.org/10.5194/essd-14-491-2022>.
- Kumar, V., Giannoukos, S., Haslett, S.L., Tong, Y., Singh, A., Bertrand, A., Lee, C.P., Wang, D.S., Bhattu, D., Stefanelli, G., Dave, J.S., Puthussery, J.V., Qi, L., Vats, P., Rai, P., Casotto, R., Satish, R., Mishra, S., Pospisilova, V., Mohr, C., Bell, D.M., Ganguly, D., Verma, V., Rastogi, N., Baltensperger, U., Tripathi, S.N., Prévôt, A.S.H., Slowik, J.G., 2022. Highly time-resolved chemical speciation and source apportionment of organic aerosol components in Delhi, India, using extractive electrospray ionization mass spectrometry. *Atmos. Chem. Phys.* 22, 7739–7761. <https://doi.org/10.5194/acp-22-7739-2022>.
- Lanz, V.A., Alfarra, M.R., Baltensperger, U., Buchmann, B., Hueglin, C., Prévôt, A.S.H., 2007. Source apportionment of submicron organic aerosols at an urban site by factor analytical modelling of aerosol mass spectra. *Atmos. Chem. Phys.* 7, 1503–1522. <https://doi.org/10.5194/acp-7-1503-2007>.
- Leaith, W.R., Macdonald, A.M., Brickell, P.C., Liggio, J., Sjostedt, S.J., Vlasenko, A., Bottenheim, J.W., Huang, L., Li, S.-M., Liu, P.S.K., Toom-Sauntry, D., Hayden, K.A., Sharma, S., Shantz, N.C., Wiebe, H.A., Zhang, W., Abbott, J.P.D., Slowik, J.G., Chang, R.Y.W., Russell, L.M., Schwartz, R.E., Takahama, S., Jayne, J.T., Ng, N.L., 2011. Temperature response of the submicron organic aerosol from temperate forests. *Atmos. Environ.* 45, 6696–6704. <https://doi.org/10.1016/j.atmosenv.2011.08.047>.
- Ma, J., Ungeheuer, F., Zheng, F., Du, W., Wang, Y., Cai, J., Zhou, Y., Yan, C., Liu, Y., Kulmala, M., Daellenbach, K.R., Vogel, A.L., 2022. Nontarget screening exhibits a seasonal cycle of PM2.5 organic aerosol composition in Beijing. *Environ. Sci. Technol.* 56, 7017–7028. <https://doi.org/10.1021/acs.est.1c06905>.
- Mehra, A., Canagaratna, M., Bannan, T.J., Worrall, S.D., Bacak, A., Priestley, M., Liu, D., Zhao, J., Xu, W., Sun, Y., Hamilton, J.F., Squires, F.A., Lee, J., Bryant, D.J., Hopkins, J.R., Elzein, A., Budisulistiorini, S.H., Cheng, X., Chen, Q., Wang, Y., Wang, L., Stark, H., Krechmer, J.E., Brean, J., Slater, E., Whalley, L., Heard, D., Ouyang, B., Acton, W.J.F., Hewitt, C.N., Wang, X., Fu, P., Jayne, J., Worsnop, D., Allan, J., Percival, C., Coe, H., 2021. Using highly time-resolved online mass spectrometry to examine biogenic and anthropogenic contributions to organic aerosol in Beijing. *Faraday Discuss* 226, 382–408. <https://doi.org/10.1039/D0FD00080A>.
- Mihara, T., Mochida, M., 2011. Characterization of solvent-extractable organics in urban aerosols based on mass spectrum analysis and hygroscopic growth measurement. *Environ. Sci. Technol.* 45, 9168–9174. <https://doi.org/10.1021/es201271w>.
- Moschos, V., Dzepina, K., Bhattu, D., Lamkaddam, H., Casotto, R., Daellenbach, K.R., Canonaco, F., Rai, P., Aas, W., Becagli, S., Calzolari, G., Eleftheriadis, K., Moffett, C. E., Schnelle-Kreis, J., Severi, M., Sharma, S., Skov, H., Vestenius, M., Zhang, W., Hakola, H., Hellén, H., Huang, L., Jaffrezo, J.-L., Massling, A., Nøjgaard, J.K., Petäjä, T., Popovicheva, O., Sheesley, R.J., Traversi, R., Yttri, K.E., Schmale, J., Prévôt, A.S.H., Baltensperger, U., El Haddad, I., 2022. Equal abundance of summertime natural and wintertime anthropogenic Arctic organic aerosols. *Nat. Geosci.* 15, 196–202. <https://doi.org/10.1038/s41561-021-00891-1>.
- Nenes, A., Pandis, S.N., Pilinis, C., 1998. ISORROPIA: a new thermodynamic equilibrium model for multiphase multicomponent inorganic aerosols. *Aquat. Geochim.* 4, 123–152. <https://doi.org/10.1023/A:1009604003981>.

- Ng, N.L., Herndon, S.C., Trimborn, A., Canagaratna, M.R., Croteau, P.L., Onasch, T.B., Sueper, D., Worsnop, D.R., Zhang, Q., Sun, Y.L., Jayne, J.T., 2011. An Aerosol Chemical Speciation Monitor (ACSM) for routine monitoring of the composition and mass concentrations of ambient aerosol. *Aerosol Sci. Tech.* 45, 770–784. <https://doi.org/10.1080/02786826.2011.560211>.
- Ostro, B., Tobias, A., Querol, X., Alastuey, A., Amato, F., Pey, J., Pérez, N., Sunyer, J., 2011. The effects of particulate matter sources on daily mortality: a case-crossover study of Barcelona, Spain. *Environ. Health Perspect.* 119, 1781–1787. <https://doi.org/10.1289/ehp.1103618>.
- Paatero, P., 1999. The multilinear engine—a table-driven, least squares program for solving multilinear problems, including the n-way parallel factor analysis model. *J. Comput. Graph Stat.* 8, 854–888. <https://doi.org/10.1080/10618600.1999.10474853>.
- Paatero, P., Tapper, U., 1994. Positive matrix factorization: a non-negative factor model with optimal utilization of error estimates of data values. *Environment (Wash. D C)* 5, 111–126. <https://doi.org/10.1002/env.3170050203>.
- Paglionie, M., Saarikoski, S., Carbone, S., Hillamo, R., Facchini, M.C., Finessi, E., Giulianelli, L., Carbone, C., Fuzzi, S., Moretti, F., Tagliavini, E., Swietlicki, E., Eriksson Stenström, K., Prévôt, A.S.H., Massoli, P., Canagaratna, M., Worsnop, D., Decesari, S., 2014. Primary and secondary biomass burning aerosols determined by proton nuclear magnetic resonance (H-NMR) spectroscopy during the 2008 EUCAARI campaign in the Po Valley (Italy). *Atmos. Chem. Phys.* 14, 5089–5110. <https://doi.org/10.5194/acp-14-5089-2014>.
- Paglionie, M., Gilardoni, S., Rinaldi, M., Decesari, S., Zanca, N., Sandrini, S., Giulianelli, L., Bacco, D., Ferrari, S., Poluzzi, V., Scotto, F., Trentini, A., Poulain, L., Herrmann, H., Wiedensohler, A., Canonaco, F., Prévôt, A.S.H., Massoli, P., Carbone, C., Facchini, M.C., Fuzzi, S., 2020. The impact of biomass burning and aqueous-phase processing on air quality: a multi-year source apportionment study in the Po Valley, Italy. *Atmos. Chem. Phys.* 20, 1233–1254. <https://doi.org/10.5194/acp-20-1233-2020>.
- Pietrogrande, M.C., Bacco, D., Visentin, M., Ferrari, S., Casali, P., 2014a. Polar organic marker compounds in atmospheric aerosol in the Po Valley during the Supersito campaigns — Part 2: seasonal variations of sugars. *Atmos. Environ.* 97, 215–225. <https://doi.org/10.1016/j.atmosenv.2014.07.056>.
- Pietrogrande, M.C., Bacco, D., Visentin, M., Ferrari, S., Poluzzi, V., 2014b. Polar organic marker compounds in atmospheric aerosol in the Po Valley during the Supersito campaigns — Part 1: low molecular weight carboxylic acids in cold seasons. *Atmos. Environ.* 86, 164–175. <https://doi.org/10.1016/j.atmosenv.2013.12.022>.
- Putaud, J.P., Van Dingenen, R., Alastuey, A., Bauer, H., Birmili, W., Cyrys, J., Flentje, H., Fuzzi, S., Gehrig, R., Hansson, H.C., Harrison, R.M., Herrmann, H., Hiltnerberger, R., Hüglin, C., Jones, A.M., Kasper-Giebl, A., Kiss, G., Kousa, A., Kuhlbusch, T.A.J., Löschau, G., Maenhaut, W., Molnar, A., Moreno, T., Pekkanen, J., Perrino, C., Pitz, M., Puxbaum, H., Querol, X., Rodriguez, S., Salma, I., Schwarz, J., Smolik, J., Schneider, J., Spindler, G., ten Brink, H., Tursic, J., Viana, M., Wiedensohler, A., Raes, F., 2010. A European aerosol phenomenology – 3: physical and chemical characteristics of particulate matter from 60 rural, urban, and roadside sites across Europe. *Atmos. Environ.* 44, 1308–1320. <https://doi.org/10.1016/j.atmosenv.2009.12.011>.
- Qi, L., Chen, M., Stefanelli, G., Pospisilova, V., Tong, Y., Bertrand, A., Hueglin, C., Ge, X., Baltensperger, U., Prévôt, A.S.H., Slowik, J.G., 2019. Organic aerosol source apportionment in Zurich using an extractive electrospray ionization time-of-flight mass spectrometer (EESI-TOF-MS) – Part 2: biomass burning influences in winter. *Atmos. Chem. Phys.* 19, 8037–8062. <https://doi.org/10.5194/acp-19-8037-2019>.
- Qi, L., Vogel, A.L., Esmaeilirad, S., Cao, L., Zheng, J., Jaffrezo, J.L., Fermo, P., Kasper-Giebl, A., Daellenbach, K.R., Chen, M., Ge, X., Baltensperger, U., Prévôt, A.S.H., Slowik, J.G., 2020. A 1-year characterization of organic aerosol composition and sources using an extractive electrospray ionization time-of-flight mass spectrometer (EESI-TOF). *Atmos. Chem. Phys.* 20, 7875–7893. <https://doi.org/10.5194/acp-20-7875-2020>.
- Ramboll, 2018. User's Guide: the Comprehensive Air Quality Model with Extensions (CAMx) Version 6.5. California.
- Sun, Y., Xu, W., Zhang, Q., Jiang, Q., Canonaco, F., Prévôt, A.S.H., Fu, P., Li, J., Jayne, J., Worsnop, D.R., Wang, Z., 2018. Source apportionment of organic aerosol from 2-year highly time-resolved measurements by an aerosol chemical speciation monitor in Beijing, China. *Atmos. Chem. Phys.* 18, 8469–8489. <https://doi.org/10.5194/acp-18-8469-2018>.
- Thorpe, A., Harrison, R.M., 2008. Sources and properties of non-exhaust particulate matter from road traffic: a review. *Sci. Total Environ.* 400, 270–282. <https://doi.org/10.1016/j.scitotenv.2008.06.007>.
- Thurston, G.D., Spengler, J.D., 1985. A quantitative assessment of source contributions to inhalable particulate matter pollution in metropolitan Boston. *Atmos. Environ.* 19, 9–25. [https://doi.org/10.1016/0004-6981\(85\)90132-5](https://doi.org/10.1016/0004-6981(85)90132-5).
- Tong, Y., Pospisilova, V., Qi, L., Duan, J., Gu, Y., Kumar, V., Rai, P., Stefanelli, G., Wang, L., Wang, Y., Zhong, H., Baltensperger, U., Cao, J., Huang, R.J., Prévôt, A.S.H., Slowik, J.G., 2021. Quantification of solid fuel combustion and aqueous chemistry contributions to secondary organic aerosol during wintertime haze events in Beijing. *Atmos. Chem. Phys.* 21, 9859–9886. <https://doi.org/10.5194/acp-21-9859-2021>.
- Valavanidis, A., Fiotakis, K., Vlachogianni, T., 2008. Airborne particulate matter and human health: toxicological assessment and importance of size and composition of particles for oxidative damage and carcinogenic mechanisms. *J. Environ. Sci. Health: Chimia* 26, 339–362. <https://doi.org/10.1080/10590500802494538>.
- Vicente, E.D., Duarte, M.A., Calvo, A.I., Nunes, T.F., Tarelho, L.A.C., Custódio, D., Colombi, C., Gianelle, V., Sanchez de la Campa, A., Alves, C.A., 2015. Influence of operating conditions on chemical composition of particulate matter emissions from residential combustion. *Atmos. Res.* 166, 92–100. <https://doi.org/10.1016/j.atmosres.2015.06.016>.
- Vlachou, A., Daellenbach, K.R., Bozzetti, C., Chazéau, B., Salazar, G.A., Szidat, S., Jaffrezo, J.L., Hueglin, C., Baltensperger, U., Haddad, I.E., Prévôt, A.S.H., 2018. Advanced source apportionment of carbonaceous aerosols by coupling offline AMS and radiocarbon size-segregated measurements over a nearly 2-year period. *Atmos. Chem. Phys.* 18, 6187–6206. <https://doi.org/10.5194/acp-18-6187-2018>.
- Wang, X., Hayeck, N., Brüggemann, M., Yao, L., Chen, H., Zhang, C., Emmelin, C., Chen, J., George, C., Wang, L., 2017. Chemical characteristics of organic aerosols in Shanghai: a study by ultrahigh-performance liquid chromatography coupled with orbitrap mass spectrometry. *J. Geophys. Res. Atmos.* 122 (11), 703–711. <https://doi.org/10.1002/2017JD026930>, 722.
- Watson, J.G., 1984. Overview of receptor model principles. *J. Control. Assoc.* 34, 619–623. <https://doi.org/10.1080/00022470.1984.10465780>.
- Zorn, S.R., Drewnick, F., Schott, M., Hoffmann, T., Borrmann, S., 2008. Characterization of the South Atlantic marine boundary layer aerosol using an aerodyne aerosol mass spectrometer. *Atmos. Chem. Phys.* 8, 4711–4728. <https://doi.org/10.5194/acp-8-4711-2008>.
- Zotter, P., Ciobanu, V.G., Zhang, Y.L., El-Haddad, I., Macchia, M., Daellenbach, K.R., Salazar, G.A., Huang, R.J., Wacker, L., Hueglin, C., Piazzalunga, A., Fermo, P., Schwikowski, M., Baltensperger, U., Szidat, S., Prévôt, A.S.H., 2014. Radiocarbon analysis of elemental and organic carbon in Switzerland during winter-smog episodes from 2008 to 2012 – Part 1: source apportionment and spatial variability. *Atmos. Chem. Phys.* 14, 13551–13570. <https://doi.org/10.5194/acp-14-13551-2014>.